



## Review article

Marcell Kiss\*, Sichen Mi, Gergely Huszka and Niels Quack

# Diamond diffractive optics—recent progress and perspectives

<https://doi.org/10.1515/aot-2020-0052>

Received August 31, 2020; accepted October 13, 2020;  
published online December 3, 2020

**Abstract:** Diamond is an exceptional material that has recently seen a remarkable increase in interest in academic research and engineering since high-quality substrates became commercially available and affordable. Exploiting the high refractive index, hardness, laser-induced damage threshold, thermal conductivity and chemical resistance, an abundance of applications incorporating ever higher-performance diamond devices has seen steady growth. Among these, diffractive optical elements stand out—with progress in fabrication technologies, micro- and nano-fabrication techniques have enabled the creation of gratings and diffractive optical elements with outstanding properties. Research activities in this field have further been spurred by the unique property of diamond to be able to host optically active atom scale defects in the crystal lattice. Such color centers allow generation and manipulation of individual photons, which has contributed to accelerated developments in engineering of novel quantum applications in diamond, with diffractive optical elements amidst critical components for larger-scale systems. This review collects recent examples of diffractive optical devices in diamond, and highlights the advances in manufacturing of such devices using micro- and nano-fabrication techniques, in contrast to more traditional methods, and avenues to explore diamond diffractive optical elements for emerging and future applications are put in perspective.

**Keywords:** diamond; diffractive optics; microfabrication.

## 1 Introduction

Diamond has always been recognized as a truly exceptional material, valued traditionally as gemstone for its unique optical appearance. Skillfully cut and polished, diamonds exhibit breath-taking colorful reflections, giving rise to their famous internal fire. The mechanical properties, such as extreme hardness, combined with excellent thermal conductivity and extraordinary resistance to chemical treatments, have further contributed to the reputation of diamond as a material above all. These outstanding properties, among others, make diamond at the same time a material of prime interest for the fabrication of optical and photonic components.

The recent technology advances in the production of synthetic diamond by chemical vapor deposition over the past decades [1] and the resulting commercial availability of high-quality diamond substrates have further accelerated research and development activities in diamond micro-optics and photonics. However, hardness and chemical inertness render precision machining of optical components in diamond by traditional methods, such as turning or ruling, notoriously challenging, if not impossible. Laser cutting and structuring [2] or diamond growth in prefabricated molds [3], have thus hitherto been the methods of choice to shape micro-optical components in diamond. Niche applications specifically exploit the outstanding material properties successfully, such as Raman lasers [4], transparent heat sinks for lasers [5] and laser windows [6]. Nevertheless, these techniques present typically dimensional control limited to micrometers and render them impractical for high-quality diffractive optical elements in the visible spectrum.

Recently, microfabrication methods including patterning by lithography and reactive ion etching, have been explored for the micro- and nanostructuring of diamond, and have since been proven to provide an avenue to manufacture features in diamond with unprecedented precision, allowing structural control well below the operating wavelength. The avenue of precision control and the prospect of exploring color center defects in single crystal diamond, e.g., as single photon emitters, has

\*Corresponding author: Marcell Kiss, EPFL, STI IMT GR-QUA, Lausanne, Switzerland, E-mail: marcell.kiss@epfl.ch. <https://orcid.org/0000-0001-5930-1367>

Sichen Mi, Gergely Huszka and Niels Quack, EPFL, STI IMT GR-QUA, Lausanne, Switzerland. <https://orcid.org/0000-0001-5189-0929> (N. Quack)

attracted considerable attention for emerging fields such as diamond photonic integrated circuits and diamond quantum photonics. Dedicated review articles on Quantum Information Processing with Diamond [7], Color Centers in Diamond [8, 9] and Integrated Photonics in Diamond [10], provide an excellent overview of the current state of the art in the respective areas of research.

At the same time, the dimensional control of features in diamond at the nanometer scale, enables the precision manufacturing of diffractive optical elements from the ultraviolet to the infrared spectrum. Consequently, this review article aims at providing an overview of the current state of the art in experimentally demonstrated diffractive optics in diamond. We first provide an overview of currently available diamond materials, followed by a summary of selected substrate preparation and relevant microstructuring methods for diamond. The subsequent review section provides an extensive overview of hitherto experimentally demonstrated diffractive optical elements in diamond, followed by a discussion, which aims at providing a quantitative comparison and perspectives for future applications.

## 2 Diamond substrates and material properties

For the large-scale manufacturing of optical devices in diamond, substrates in high quality and reasonable fabrication cost are required. Synthetic diamond can today be produced in quantities and with controllable material properties. Diamond substrates for optical devices can be classified in two major categories: single-crystal diamond (SCD) or polycrystalline diamond (PCD).

Single-crystal substrates are fabricated by either high-pressure high-temperature processes [11] or grown by chemical vapor deposition (CVD) on single-crystal seeds [12]. They can be manufactured with high purity, presenting a low density of defects, resulting in well-controlled optical properties such as low absorption. However, due to the single-crystalline growth method, they are typically limited in size. Today, commercial offerings of single crystal diamond substrates are in the range of  $2\text{ mm} \times 2\text{ mm}$  up to  $10\text{ mm} \times 10\text{ mm}$ , with a thickness ranging from several  $10\text{ }\mu\text{m}$  up to several millimeters. Larger single-crystal substrates take significant time to grow and require large reactors or anvils, dramatically increasing the manufacturing cost.

Polycrystalline diamond substrates can be grown or deposited by chemical vapor deposition on a variety of different substrates, such as silicon or glass wafers, and unlike SCD growth do not require single-crystal diamond seeds. PCD substrate growth can be a significantly faster

process, and can even be grown on templates, shaping the diamond layer in a single step. However, as the denomination suggests, the microstructure of deposited or grown films or substrates is polycrystalline. Depending on the deposition process parameters, the resulting films can be categorized by crystal grain size, such as micro-, nano- or ultrananocrystalline diamond films [13]. The material properties depend in general on the microcrystalline structure. For example, the grain boundaries and interfaces, as well as the resulting surface after growth exhibiting various crystal orientations, act as local scattering sites in optical components, and the polycrystalline microstructure can thus impact the optical performance dramatically, for example leading to increased optical losses.

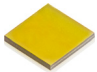
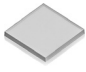
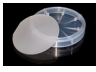



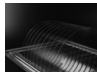
The material properties of both single- and polycrystalline diamond substrates depend on the purity of atomic constituents. Impurities are resulting during growth, by incorporation of atoms such as nitrogen or silicon, replacing carbon atoms in the crystal lattice or introducing more complex defects such as nitrogen-vacancy or silicon-vacancy centers. The inclusion of impurity atoms in the grown crystal will affect the absorption spectrum, and for optical control of the material, it is thus in general desirable to reduce the amount of impurities in diamond substrates. However, particular applications can benefit of intentional doping of diamond, such as by incorporating various atoms (N, Si) to produce color centers [14, 15] or doping with boron to create conductive diamond films [16].

Among the most attractive optical properties of diamond is the high refractive index (2.4 at 635 nm [17]), combined with a low absorption over a wide spectral range spanning from ultraviolet to far infrared [18]. Furthermore, diamond exhibits high thermal conductivity up to  $2200\text{ W/m K}$  [19], which contributes to a remarkably high laser-induced damage threshold for optical components,  $20\times$  better than fused silica in certain conditions [20]. These properties uniquely enable compact, high power laser components and spectrometers operating in the visible and UV range that are not immediately accessible with other materials.

A selection of typical diamond substrates both in single-crystalline and polycrystalline material structures are summarized in Table 1, including their material properties of relevance for diffractive optical elements, and compared to commonly employed materials silicon, sapphire and silica. Only the most relevant material parameters for diffractive optics in diamond are summarized here, an extensive digest on the properties of diamond can be found in the study by Zaitsev [18].

Since as-grown or laser-cut diamond substrates present significant surface roughness [29, 30], polishing is indispensable before further micro- and nanofabrication

**Table 1:** Diamond substrates and their key material properties for diamond diffractive optics.

	 SCD [N] <sup>a</sup>	 SCD <sup>a</sup>	 SCD [B] [21]	 PCD <sup>a</sup>	 Silicon <sup>b</sup>	 Sapphire <sup>c</sup>	 Silica <sup>d</sup>
Refractive index (1550 nm)		2.3878 [22]			3.5167 [23]	1.7462 [24]	1.444 [25]
Transparency window ( $\mu\text{m}$ )		0.22–20 [19]			1.1–6.5 [19]	0.17–5.5 [19]	0.38–2.2 [19]
Hardness (GPa)		50–110 [19]			13 [26]	15.6–17.4 [19]	7.8–8.8 [27]
Thermal conductivity ( $\text{W m}^{-1} \text{K}$ )		2200 [19]			140 [19]	24 [19]	10 [19]
Young's modulus (GPa)		1080–1155 [28]			162 [19]	340 [19]	95 [19]

In comparison to more traditional materials for micro-optical components such as silicon, sapphire or silica, diamond exhibits superior hardness, thermal conductivity and Young's modulus, with an extremely broad transparency window and high refractive index. SCD, single-crystal diamond; PCD, polycrystalline diamond. <sup>a</sup>Image used with permission of Element Six Group, Copyright © Element Six Group, 2020. <sup>b</sup>Image used with permission of SIEGERT WAFER GmbH. <sup>c</sup>Image used with permission of MTI Corporation. <sup>d</sup>Image used with permission of SCHOTT AG.

processing. Diamond polishing is performed either mechanically or via contactless etching, typically reactive ion etching or ion beam etching with inert-gas ions, or in a combination of both [31, 32]. In order to achieve optical quality, the surface roughness required for small scattering loss is typically less than 1/10 of the operating wavelength. For optical components for the infrared and longer wavelengths, mechanically polished PCD substrates are in general sufficiently smooth [33]. For optical components for the UV–Visible range, SCD substrates are preferred as they manifest much lower material absorption, however, mechanical polishing of SCD can be problematic due to a strong anisotropy of the polishing rate, which can result in undesired surface roughness with abundant polishing pits [32, 34].

Along carefully chosen crystallographic directions, mechanical polishing with a scaif is able to give subnanometer smooth SCD surface, but this approach applies only to small substrates (typically limited to 3–8 mm) with sufficient thickness (>50–200  $\mu\text{m}$  depending on the area) as the substrate otherwise would be easily broken [35]. To counter this difficulty, noncontact polishing methods via chemical or physical etching are developed to provide a new route [31, 32, 36, 37]. In particular, ion beam polishing has been demonstrated as a fast, affordable and scalable approach to give subnanometer smooth surface with peak-to-valley value less than  $\lambda/100$  for UV–Visible optics [32], and we have employed this method in manufacturing a variety of DOEs with different design routes [38–40].

### 3 Diamond micro- and nanofabrication

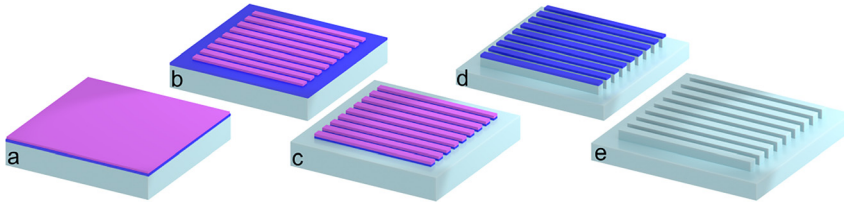
Traditional machining methods for diffractive optics include mechanical ruling or turning, where material is removed from a substrate using a diamond tool, creating the

diffractive relief pattern [41]. However, due to the hardness and chemical resistance, these traditional methods are generally not applicable for the fabrication of diffractive optical components in diamond. For diffractive optics fabricated out of resin, molding can be a competitive fabrication method [42]. A closely related method to molding consists in template growth, which has been employed with success for polycrystalline diamond [3, 33]. A growth substrate (such as a silicon wafer) is shaped (e.g. by wet or reactive ion etching) to mimic the inverse profile of the final device. The polycrystalline diamond layer is subsequently grown on the template, and upon detaching of the template, freestanding diamond structures are obtained.

Laser cutting is a suitable technique for manufacturing micro-optics, but does not achieve the required precision for DOEs [43], while surface modification and localized graphitization are alternative promising techniques [2].

The drive to smaller feature sizes, tolerances and shorter wavelengths require more precise techniques, which are enabled by microfabrication methods. Diamond microfabrication builds on the decades of experience in microfabrication with other substrates, in particular for silicon and glass wafers. In this section, we briefly outline the most commonly employed techniques for diamond microfabrication. Compared to traditional methods, microfabrication provides more flexibility and precision, and can be parallelized to large-scale wafer-level fabrication.

A generalized microfabrication process to manufacture a diffractive optical element in diamond by micro- and nanofabrication methods, is schematically depicted in Figure 1. The process is referred to as bulk micromachining and involves several steps. First, a masking layer is deposited on top of the diamond surface, which in turn is covered by a resist. Exposure of a pattern on the resist and development allows to transfer a design into the resist. Subsequently, both the masking layer and the diamond are selectively etched.



**Figure 1:** Generalized process flow for diamond microfabrication, based on bulk micromachining and photolithography. (a) Hardmask and photoresist are deposited onto the diamond substrate. (b) The photoresist is exposed with desired pattern. (c) The pattern is transferred into the hardmask. (d) The hardmask is used to etch the same pattern into the diamond bulk. (e) The hardmask is stripped, revealing the final relief in the diamond.

Pattern creation methods depend on the critical dimension required for the structure—photolithography techniques are limited by the wavelength used, which is on the order of  $0.8\ \mu\text{m}$ – $1\ \mu\text{m}$  for UV lithography and  $100$ – $200\ \text{nm}$  for deep UV steppers. Features below this size are realized using electron beam lithography, which can achieve nanometer-scale resolution. Some techniques also exist that take advantages of a high-resolution pattern prepared on a template in advance, such as imprint lithography [44]. 2.5D structures can be created using 2-photon lithography [40]. For diffractive structures, special techniques can prove successful, such as interference lithography [45] and Talbot lithography [46], which are uniquely suited to produce periodic structures.

Diamond etching is a challenging endeavor as diamond is exceptionally chemically resistant—hence wet chemical etching is extremely challenging. Diamond etching is thus typically achieved using dry processes—primarily plasma etching. The preferred etching gas is oxygen, facilitating the removal of carbon atoms from the surface as  $\text{CO}_x$  byproducts, but alternative processes employ chlorine or fluorine chemistry as well. In general, it has been found that the addition of oxygen increases etch speed, while other gases help to maintain a smooth etch floor. The need to use aggressive etches decreases the selectivity between the mask material and the diamond, which leads to the use of hard masks (an additionally deposited thin film) instead of photoresist masks for many processes. Typical hardmasks include  $\text{SiO}_2$ , Al and  $\text{Al}_2\text{O}_3$  films, with selectivity to the masking material 1:50 or less. A comprehensive review on the different etch processes, hardmasks, selectivities and etch results can be found in the study by Toros et al. [47].

Figure 2 provides an overview of typical critical target dimensions for diffractive optical elements as function of their operating wavelength, along with the preferred lithography techniques. The scanning electron microscopy (SEM) images show representative fabricated structures, which are discussed in the following section.

## 4 Review of diffractive optical elements in diamond

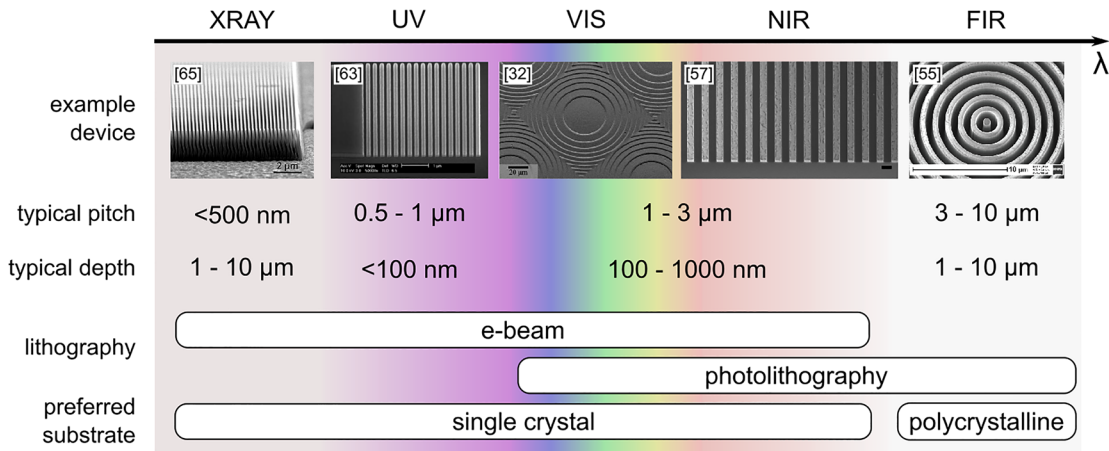
The manufacturing of diffractive optical elements in diamond poses stringent requirements on the pattern definition (Figure 2). The requirements on the dimensional control become increasingly challenging with decreasing operating wavelength. In the following, experimentally demonstrated diffractive optical elements are summarized, accordingly in order from long wavelength devices for the infrared to short wavelength devices for X-rays.

### 4.1 Far- and mid-infrared

The fabrication of long wavelength devices exploring the generalized manufacturing process presented in Figure 1, have been explored for optical elements for high-power  $\text{CO}_2$  lasers. In this context, diffractive structures are particularly useful as antireflection layers in combination with other optical elements. A subwavelength periodic structure is formed, which acts as a modulation of refractive index, creating an index gradient between diamond and air, suppressing Fresnel reflections in a wavelength-dependent way. Karlsson et al. [48] fabricated antireflection structured surfaces for the infrared spectral region. Sputtered Al was patterned using e-beam lithography and etched using chlorine chemistry ICP RIE. The definition of the antireflection layer increases transmission from 71% to 97% when applied on both sides, for an illuminating wavelength of  $10.6\ \mu\text{m}$  (typical for  $\text{CO}_2$  lasers).

Fu and Ngoi [49] fabricated diffractive elements in a polycrystalline  $1.5\text{-}\mu\text{m}$  thick diamond film on fused silica, using a dedicated 50 keV Ga focused ion beam milling process. The authors report a diffraction efficiency of 73%, and remark that the fabrication of one DOE structure takes  $\sim 20\ \text{min}$ .





**Figure 2:** Graphical guideline for the choice of fabrication processes for diamond diffractive optical elements organized by operating wavelength, with illustrations of demonstrated example devices. For high performance diffractive optical elements at short wavelengths, single crystal diamond substrates and e-beam lithography are the preferred substrates and lithography methods of choice, while polycrystalline substrates and photolithography are suitable techniques for longer operating wavelengths, where photolithography summarizes the various techniques such as contact, interference, DUV, Talbot lithography and 2-photon absorption lithography.

Anti-Reflection (AR) layers were also fabricated by Martínez-Calderon et al. [51] using laser-induced periodic surface structuring via femtosecond laser pulses. Nanostructuring was carried out by pulsed laser light at different wavelengths, resulting in grooves of different morphologies. According to modeling carried out by the authors, these patterns can raise transmission by 12% compared to an unstructured surface.

Diffractive optical elements for shaping and transforming beams have been demonstrated by Karlsson et al. [52] in binary DOE fabricated in polycrystalline diamond, designed as a fan-out element (16-way beamsplitter). Sputtered Al was patterned via contact photolithography. The diamond etch was carried out in Ar/O<sub>2</sub> plasma, with an etch depth of 3.84  $\mu\text{m}$  (for 10.6  $\mu\text{m}$  operation) or 224 nm (for 633 nm operation). Uniformity error of 4% is reported for red light.

High aspect ratio gratings were fabricated by Forsberg and Karlsson [50]. Thick aluminum is used as hard mask that masks against strongly biased Ar/O<sub>2</sub> plasma. The process employs multiple hardmask layers and pattern transfers to create the desired Al hardmask. A critical problem addressed with this method is the erosion of the mask layer during the aggressive diamond etch step. The hardmask geometry undergoes evolution during etching that leads to faceting, which accelerates the erosion due to the increased sputtering yield of the lower angles, eventually receding from the edges of the diamond bar. To combat this effect, the mask layer thickness is increased to 1.7  $\mu\text{m}$ , which enables 13.7  $\mu\text{m}$  deep grooves in the diamond. The article also elaborates on the bottom surface

roughness as a function of initial hardmask geometry: it is observed that vertical sidewalls prevent micromasking from the resputtering of the hardmask. When the hardmask has become faceted, the redeposition occurs, but the etch floor is no longer in line-of-sight for the sputtered atoms.

The grating fabrication technique was subsequently refined by Vargas Catalan et al. [53]. Fabrication was carried out in polycrystalline diamond, with a hardmask stack similar to previous work [50]. Solvent-assisted micro-contact molding is used to define the grating patterns in the hardmask stack. A Si master is patterned using e-beam lithography, used to fabricate a PDMS stamp. Photoresist (PR) is coated onto the diamond with the hardmask, and the stamp is positioned on top of the resist. The substrate is placed into solvent-saturated atmosphere (ethanol), which permeates the PDMS stamp. The PR softens, and fills the patterns in the stamp due to capillary forces, which is then used to pattern the hardmask and subsequently the diamond substrate. Optimization of the etch parameters results in the control of the sidewall angle between 2.1° and 4.2°. The authors demonstrate greater control of the maximum etch depth by periodically resputtering the Al hardmask. Due to shadowing, the Al layer is thicker at the top of the groove, than at the bottom. A short etch is able to remove the mask material from the bottom of the groove, enabling the continuation of the etch process. An aspect ratio of 1:13.5 and a sidewall angle of 1.55° is demonstrated with this approach. Half-wave plates are also demonstrated for the mid-IR by Delacroix et al. [54]. Sub-wavelength gratings were optimized to work in the N-band (8–13  $\mu\text{m}$ ). The design employs gratings of trapezoidal

profile, that were optimized to be tolerant of fabrication errors. An antireflective grating was fabricated on the backside to decrease transmission losses. The fabricated structures show increased transmission compared to the original plate (89–95%), along with a retardance of  $(180.08 \pm 3.51)^\circ$  over the N-band.

Similar fabrication was shown for quarter-wave plates by Forsberg et al. [55]. In addition, free-hanging gratings are fabricated in a polycrystalline diamond thin film on silicon. After the patterning of the diamond layer using ICP RIE, the underlying Si bulk is etched in a modified anisotropic Si etch, that undercuts the grating, leaving it free-hanging in a silicon frame. Crossbars were added to the grating lines to enforce buckling in the same direction. The authors note that a free-hanging grating can be advantageous in reducing transmission losses (no bulk Fresnel losses/no AR layer needed), a less demanding fabrication (without a large index substrate, the grating lines can have a larger period while retaining subwavelength properties) and better production scalability but the resulting devices are more fragile and difficult to handle.

Similarly, microfabricated subwavelength gratings were demonstrated for coronagraphy imaging of objects close to a star [56]. Annular groove phase mask subwavelength gratings were fabricated for both near infrared (1–3  $\mu\text{m}$ ) and visible (400–700 nm), along with vortex phase masks with a topological charge of 4. An interesting technique shown in this article is the ability to tune the depth of gratings postfabrication. To decrease the depth of the fabricated gratings, photoresist is coated, filling the grooves. Subsequent etching decreases the groove depth,

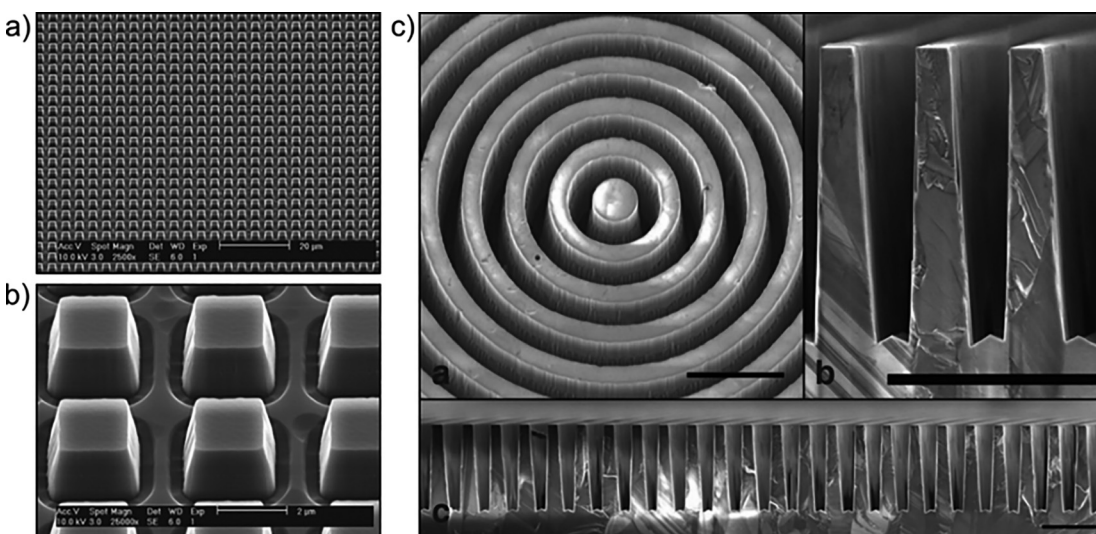
due to slower etch of the PR at the bottom of the groove. Increasing the groove depth is performed by Al resputtering, similarly to previous work [53].

Kononenko et al. [33] demonstrate far infrared ( $\text{CO}_2$  wavelength) components by a novel combination of laser microstructuring and diamond growth. A silicon template is structured using pulsed laser machining to form the inverse of the desired surface, then polycrystalline diamond is grown over the template after the template is seeded with nanodiamonds. After the desired thickness is achieved (after 496 h of growth), the top surface is polished. The silicon template is etched away and the diamond surface is etched in air to remove residual nondiamond carbon phases. The resulting structured diamond surface is smooth ( $R_a = 21 \text{ nm}$ ), which results in low scattering and the fabricated components operate close to the theoretical maximum ( $77 \pm 3\%$ , maximum: 82%). Representative examples of demonstrated diamond diffractive optical elements are shown in Figure 3.

## 4.2 Near infrared

The interest in the near infrared wavelengths is mainly motivated by applications for telecommunications, typically in the C-band at 1.55  $\mu\text{m}$  wavelength. Among the demonstrated devices are grating couplers for coupling to photonic integrated circuits and high contrast grating for high reflection devices.

Gao et al. [57] fabricate grating couplers for 1550 nm on diamond-on-insulator substrates. E-beam lithography with



**Figure 3:** Diffractive elements for the IR. (a) and (b) Antireflective microstructures (moth-eye) fabricated in polydiamond for far-IR (10.6  $\mu\text{m}$ ) [48]. (c) Circularly symmetric half-wave plates, fabricated via a hardmask resputtering-based process to maintain sidewall angle with high aspect ratios. Scale bars are 10  $\mu\text{m}$  long [50].

proximity correction is used to pattern the 950-nm pitch coupler, using a hydrogen silsesquioxane (HSQ) resist. The patterns are transferred into the diamond film using an  $O_2/Ar$  plasma. Characterization reveals a  $-6.3$  dB grating coupler loss.

Huszka et al. [58] demonstrate a high contrast grating (HCG) design that was configured to achieve higher than 95% reflectance at operating wavelength of 1550 nm into the zeroth order, which is an essential requirement for integration in vertical external cavity surface emitting laser structures. Numerical optimization was carried out to produce a design with  $>99.99\%$  reflection for the target wavelength. The single crystal diamond plates ( $3 \times 3 \times 0.25$  mm<sup>3</sup> Element Six) were polished as described in the study by Mi et al. [32]. A dual-purpose metal mask was deposited on the diamond surface in order to provide a conductive layer for e-beam lithography and a hard mask for diamond etching, patterned subsequently via an e-beam exposed HSQ resist. Using the HSQ as mask, the titanium layer was then plasma etched using  $Cl_2/BCl_3$  chemistry. The subsequent diamond etch was carried out using solely  $O_2$  plasma, with an etch rate of 90–100 nm/min. The mask was removed in 49% HF acid. The fabricated gratings were subsequently measured by SEM and AFM to confirm the geometrical shapes and dimensions. The SEM images showed well-defined structures of the extruded bars with smooth and near-vertical sidewalls, and a complete absence of micromasking, frequently encountered in diamond processing [59]. AFM measurements confirmed good agreement with target dimensions. The fabricated HCG reached 95.85% at 1550 nm wavelength, which is  $\sim 3\%$  lower than designed. This discrepancy is attributed to a combination of imperfections resulting from the fabrication process, such as surface roughness leading to scattering losses, nonverticality of the grating bars or the residual trenches observed at the bottom edges of the grating bars, and tolerances resulting from the measurement method, such as imperfect alignment of the grating with respect of the collimating lens.

### 4.3 Visible and ultraviolet

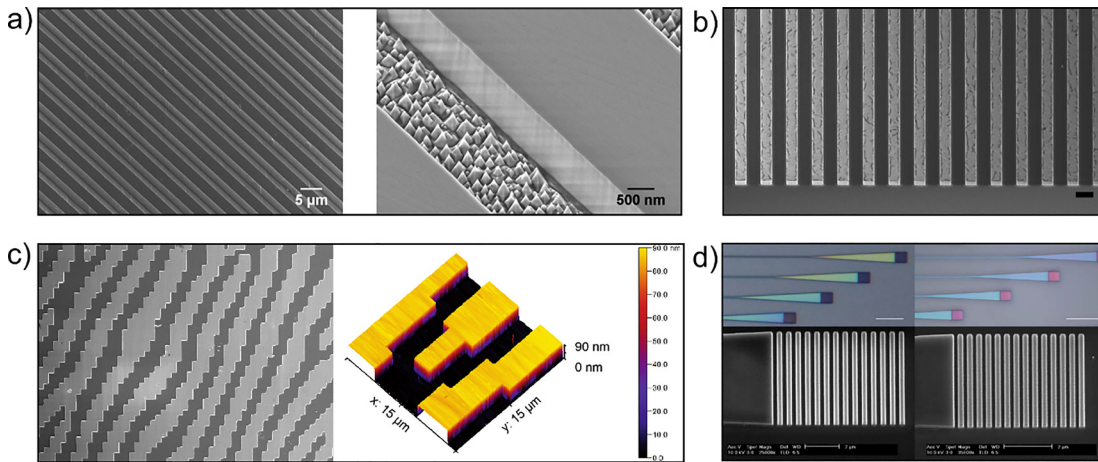
In the visible, the high refractive index and the transparency window that extends into the deep UV makes it stand out from fused silica and sapphire, enabling applications such as welding and spectrometry. Kiss et al. [38] demonstrate a novel method for fabricating single-crystal diamond diffraction gratings based on crystallographic etching. Commercially available  $\langle 100 \rangle$  diamond plates were patterned using contact lithography, with grooves

aligned to both  $\langle 100 \rangle$  and  $\langle 110 \rangle$  directions, resulting in V-groove and rectangular gratings, due to the selectivity of the etch to crystallographic planes. The resulting gratings were characterized using scanning electron microscopy and atomic force microscopy, revealing angles of  $57^\circ$  and  $87^\circ$  depending on the crystal orientation, with mean roughness below  $R_a = 5$  nm on the sidewalls. The optical performance of the gratings was simulated using RCWA [60] and compared to with measured values at 633 nm, showing good agreement. This work follows previous experiments into triangular and trapezoidal profile gratings [61, 62].

Toros et al. the fabricate high-precision 3D micro-optical components in single-crystal diamond using 3D laser lithography [40]. Fresnel microlens arrays and blazed diffraction gratings are microfabricated and characterized. The fabrication process is carried out on commercially available single-crystal diamond plates. The photoresist structures are created using layer-by-layer writing via 3D dip-in laser lithography (NanoScribe). This allows high-resolution 3D structures, which are then transferred into the substrate by a chlorine-based reactive ion etching with a low diamond:photoresist selectivity (1:15). The resulting surfaces are characterized using SEM and AFM, revealing smooth etched surfaces with a mean roughness ( $R_a$ ) smaller than 2 nm. Furthermore, this pattern transfer process faithfully reproduces the features written into the photoresist, scaled by the selectivity. The Fresnel microlenses were optically characterized using a Mach–Zehnder interferometer, showing a focal length deviation of 4% from the target value. The gratings show a relative efficiency of 66% in the first order.

An example of exploiting the unique color centers along with diffractive optics is shown by Li et al. [63]. A circular grating is patterned into the diamond surface, enclosing a nitrogen-vacancy center. The grating is used to enhance the collection of photons from the center. Pre-patterned silicon membranes were transferred to the diamond surface to use as mask during the subsequent etching, then removed. The collection efficiency is increased to 30% due to the grating.

Wildi et al. [39] demonstrate the design, fabrication and experimental characterization of near-field binary-phase transmission Diffractive Optical Elements (DOEs) in single-crystal diamond. Top-hat and arbitrary pattern DOE beam shapers were numerically optimized using an iterative Fourier transform algorithm. Commercially available single-crystal diamond plates ( $3 \times 3 \times 0.3$  mm<sup>3</sup>) were polished using ion beam etching [32]. Amorphous silicon hardmask was deposited and e-beam lithography was carried out using an HSQ mask. Chlorine-based plasma



**Figure 4:** Devices operating in the visible. (a) V-groove and vertical gratings fabricated using crystallographic etching [38]. (b) High reflectance binary grating for VCSELs [58]. (c) Top-hat forming DOE designed for 532 nm welding [39]. (d) Grating couplers for UV guided-wave optics [64].

etching was used to transfer the e-beam written patterns into the Si hardmask layer, followed by O<sub>2</sub> plasma-based diamond reactive ion etching for transferring the patterns into diamond. The hardmask was then stripped in poly-Si etch. The resulting binary phase relief patterns were characterized using SEM and atomic force microscopy (AFM), showing smooth etch floors and vertical sidewalls. Subsequently, the DOEs were experimentally in transmission at  $\lambda = 532$  nm, confirming excellent uniformity of the resulting top-hat beam profile as required in copper welding applications.

Gao et al. [64] report on the design, fabrication and experimental demonstration of SCD waveguide devices with integrated grating couplers optimized for 850, 635 and 405 nm wavelengths, respectively. The devices are fabricated on SCD thin films using electron-beam lithography and reactive-ion etching technologies. A tilted etching technique is used to produce flat diamond films suitable for guided wave fabrication. Tapered fibers are used to probe the 850 and 635 nm integrated devices, showing coupling losses of 20.6 and 22.7 dB. The waveguide losses are measured as of 11 dB mm<sup>-1</sup> and 20.5 dB mm<sup>-1</sup>. The 405 nm devices are probed instead with a lensed fiber, and show a coupling loss of 33.1 dB and a larger 46.7 dB mm<sup>-1</sup> waveguide loss.

Blazed diffraction gratings and diffractive optical elements were fabricated in polycrystalline diamond by Karlsson et al. [65] for operation at 400 nm wavelength. Continuous relief structures were exposed by electron beam lithography, which were transferred into diamond using Ar/O<sub>2</sub> ICP RIE, with a selectivity of 1:10. The authors report a smooth transferred surface, but attribute most of

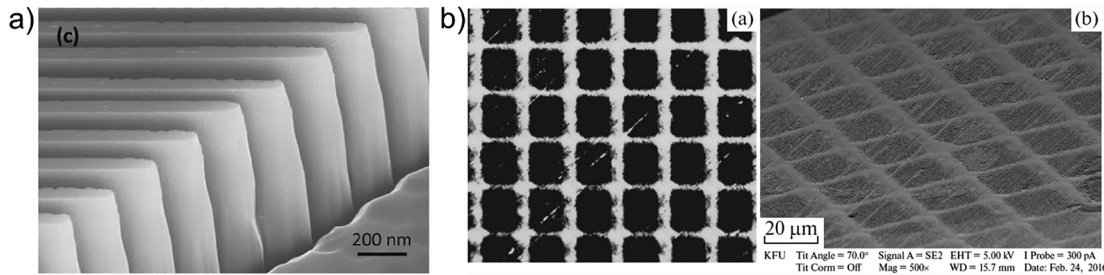
the deviation from the theoretical diffraction efficiency to deviation from the ideal resist profile. Experimentally demonstrated diamond diffractive optical elements for the visible and ultra-violet are summarized in Figure 4.

#### 4.4 X-ray

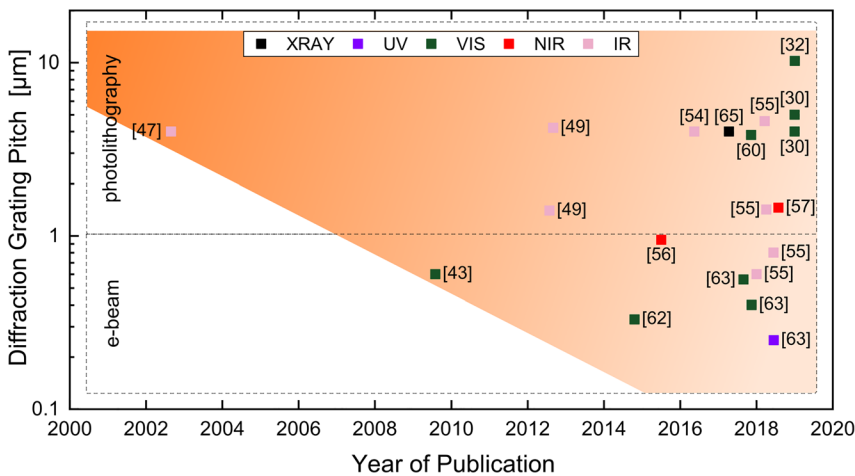
Microfabricated X-ray gratings have been demonstrated by Makita et al. [66]. A 500 nm HSQ layer is used with a chromium adhesion/conduction layer of 30 nm to create the grating patterns. The grating pattern is exposed via electron-beam lithography resulting in grating lines with 30 nm to 4 μm pitches. The etch process first transfers the electron-beam written pattern into the chromium using chlorine/oxygen chemistry, then transfer the pattern into diamond using an oxygen-based recipe. The HSQ layer is cured before diamond etching to increase recipe selectivity (300 °C, 40 min). The diamond etching is continuously tuned every 1–2 μm to maintain sidewall angle. The resulting structures have an aspect ratio between 10 and 20. Continuing this line of research, suspended gratings were fabricated by Kujala et al. [67], somewhat similarly to the free-hanging gratings previously demonstrated by Forsberg et al. [55], on a suspended CVD diamond membrane attached to a Si frame. A diffraction efficiency map of the first order was measured, indicating an efficiency variation of 20% across the whole grating. The variation is attributed to a nonflat diamond substrate, resulting in variation in the e-beam-written patterns due to focus error.

An alternative fabrication process was carried out using ion implantation as a way of graphitizing selected areas in





**Figure 5:** Gratings designed for X-ray operation. (a) E-beam patterned dense gratings fabricated a chrome hardmask [66]. (b) Selectively boron-implanted and graphitized diamond diffraction grating [68].



**Figure 6:** Comparison of selected diamond diffractive devices, based on year of publication and groove pitch, highlighting the maturing of the fabrication technology, allowing a push to smaller feature sizes. For features below 1 μm e-beam is the most suitable technology, while larger features can be written by either photolithography or e-beam. The broadening interest in this field is also shown by an increase in the number of publications in recent years. Both trends, smaller demonstrated feature sizes and increase in demonstrated applications over the past two decades, are highlighted by the shaded areas.

diamond by Stepanov et al. [68]. Boron ions with an energy of 40 keV were implanted with a high fluence of  $1.43 \times 10^{18}$  ion/cm<sup>2</sup>, masked by nickel grid with 40 μm square openings. SRIM simulation [69] indicates that the boron atoms are deposited in a ~100-nm-thick layer resulting in graphitization due to the high fluence. The graphitized layer expands due to lower density of amorphous carbon ( $\rho_{a-c} = 2.09\text{--}2.23$  g/cm<sup>3</sup>) compared to diamond ( $\rho_{\text{Diamond}} = 3.47\text{--}3.55$  g/cm<sup>3</sup>) and the refractive index changes to  $n_{a-c} = 2.1\text{--}2.223$ , thereby creating the optical path difference. An investigation into tungsten-relief and diamond-relief gratings for high energy hard X-ray diffractive optics revealed that the diamond gratings withstand a fluence of 59000 mJ/cm<sup>2</sup> at 8.2 keV, 118 × the amount measured for tungsten gratings before damage occurred [70]. The damage manifested in the diamond gratings as unintended graphitization. An innovative way of improving diffraction efficiency for diamond nanofabricated Fresnel zone plates were presented by David et al. [71]. The electron-beam lithography-structured diamond structure was filled with Ir, deposited conformally via atomic layer deposition. The high density of iridium confers an increase in phase

shifting, while the diamond fins serve as an effective way of cooling the metal to prevent damage. A representative selection of demonstrated diamond diffractive optical elements for X-ray operation is shown in Figure 5.

## 5 Discussion

As seen from the discussed exemplars of diamond diffractive devices, the field is rapidly evolving, fueled by accessible, affordable, high-quality substrates and progress in micro- and nanofabrication techniques. Over the years, the improvement in manufacturing has pushed the minimum feature size to ever smaller minimum feature sizes, resulting in devices with shorter operating wavelength, while at the same time enabling higher quality for longer wavelength elements. The progress of the field is illustrated in Figure 6, where the demonstrated diffractive optical elements are organized by feature dimension (pitch) versus the time of publication. The selection of diffractive devices showcases the evolution of diamond

diffractive devices and the push for shorter wavelengths, as well as the resulting increase in the number of published results in recent years, addressing an increased diversity of applications. Both trends, smaller demonstrated feature sizes and increase in demonstrated applications over the past two decades, are clearly visible in Figure 6 as highlighted by the shaded areas.

Future applications will be successful when diamond optics, and specifically diffractive optics can find applications where the diamond's extreme material properties can be used to add value to existing products or enable new products which were previously impossible. Diamond boasts a high refractive index, which is of interest for transmission components. Diamond-based optics can thus be built more compact, which is of interest for portable devices. This advantage is manifested primarily for visible and UV wavelengths, where silicon is not transparent. Furthermore, diamond has a high laser-induced damage threshold and the highest bulk thermal conductivity of all materials, both of which enable high power applications. Another property is diamond's extreme hardness, which means that diamond components can be subjected to significant abrasion without damaging the component. Furthermore, the chemical resistance means that parts that accumulate contaminants can be subjected to aggressive wet cleaning in acids or oxygen stripping in barrel-type plasma etcher without problem, which is an advantage for gratings operating in dusty environment or handled frequently. Chemical resistance can also open applications where, for example, an exit window for a laser needs to be submerged in a corrosive substance—this can be withstood by diamond for virtually any chemical. These properties enable new diffractive optics applications, where diamond can drive high power optics in harsh environments.

Finally, with the recent interest in exploring diamond photonics for quantum sensing and quantum information processing by exploitation of color centers in diamond, engineering and optimization of optical structures to enhance the collection efficiency of (single) photon sources can dramatically increase their performance, consequently, diamond diffractive optical elements are poised to play a vital role in performance enhancement in these emerging applications in the future.

## 6 Conclusion

This review aims to give an overview of the recent progress and current status in diffractive optical elements in diamond manufactured by micro- and nanofabrication techniques. This emerging field is rapidly growing, driven by

the accessibility of high-quality substrates, leading to applications where diamond's extreme properties can be exploited to create diffractive components that can surpass existing devices, such as for high power, exotic wavelength, harsh environment or quantum information processing devices.

**Acknowledgments:** The authors acknowledge funding by the Swiss State Secretariat for Education, Research and Innovation and by the Swiss National Science Foundation under Grants 157566 and 183717.

**Author contribution:** All the authors have accepted responsibility for the entire content of this submitted manuscript and approved submission.

**Research funding:** The authors acknowledge funding by the Swiss State Secretariat for Education, Research and Innovation and by the Swiss National Science Foundation under Grants 157566 and 183717.

**Conflict of interest statement:** The authors declare no conflicts of interest regarding this article.

## References

- [1] M. Schwander and K. Partes, "A review of diamond synthesis by CVD processes," *Diam. Relat. Mater.*, vol. 20, p. 1287, 2011.
- [2] V. Bharadwaj, O. Jedrkiewicz, J. P. Hadden, B. Sotillo, M. R. Vázquez, P. Dentella, T. T. Fernandez, A. Chiappini, A. N. Giakoumaki, T. Le Phu, M. Bollani, M. Ferrari, R. Ramponi, P. E. Barclay, and S. M. Eaton, "Femtosecond laser written photonic and microfluidic circuits in diamond," *J. Phys. Photonics*, vol. 1, p. 022001, 2019.
- [3] E. Woerner, C. Wild, W. Mueller-Sebert, and P. Koidl, "CVD-diamond optical lenses," *Diam. Relat. Mater.*, vol. 10, p. 557, 2001.
- [4] S. Reilly, V. G. Savitski, H. Liu, E. Gu, M. D. Dawson, and A. J. Kemp, "Monolithic diamond Raman laser," *Opt. Lett.*, vol. 40, p. 930, 2015.
- [5] A. Broda, A. Kuźmicz, G. Rychlik, K. Chmielewski, A. Wójcik-Jedlińska, I. Sankowska, K. Gołaszewska-Malec, K. Michalak, and J. Muszalski, "Highly efficient heat extraction by double diamond heat-spreaders applied to a vertical external cavity surface-emitting laser," *Opt. Quant. Electron.*, vol. 49, p. 287, 2017.
- [6] Diamond PureOptics, Available at: <https://asia.e6.com/en/Home/Applications/Optics/High+power+laser+optics/Diamond+PureOptics/> [accessed: August 2019].
- [7] S. Praver, and I. Aharonovich, Eds. *Quantum Information Processing with Diamond: Principles and Applications*, Amsterdam; New York, Elsevier/WP, Woodhead Publishing Is An Imprint Of Elsevier, 2014.
- [8] I. Aharonovich and E. Neu, "Diamond nanophotonics," *Adv. Opt. Mater.*, vol. 2, p. 911, 2014.
- [9] A. Chatterjee, P. Stevenson, S. De Franceschi, A. Morello, N. de Leon, and F. Kuemmeth, *Semiconductor Qubits In Practice*. [arXiv:2005.06564 [cond-mat, Physics:quant-Ph]]; 2020.

- [10] S. Mi, M. Kiss, T. Graziosi, and N. Quack, "Integrated photonic devices in single crystal diamond," *J. Phys. Photonics*, vol. 2, p. 042001, 2020.
- [11] H. Sumiya and K. Tamasaku, "Large defect-free synthetic type IIa diamond crystals synthesized via high pressure and high temperature," *Jpn. J. Appl. Phys.*, vol. 51, p. 090102, 2012.
- [12] F. Silva, J. Achard, O. Brinza, X. Bonnin, K. Hassouni, A. Anthonis, K. De Corte, and J. Barjon, "High quality, large surface area, homoepitaxial MPACVD diamond growth," *Diam. Relat. Mater.*, vol. 18, p. 683, 2009.
- [13] P. W. May and Y. A. Mankelevich, "From ultrananocrystalline diamond to single crystal diamond growth in hot filament and microwave plasma-enhanced CVD reactors: a unified model for growth rates and grain sizes," *J. Phys. Chem. C*, vol. 112, p. 12432, 2008.
- [14] I. Aharonovich, S. Castelletto, D. A. Simpson, C.-H. Su, A. D. Greentree, and S. Praver, "Diamond-based single-photon emitters," *Rep. Prog. Phys.*, vol. 74, p. 076501, 2011.
- [15] L. T. Hall, J. H. Cole, C. D. Hill, and L. C. L. Hollenberg, "Sensing of fluctuating nanoscale magnetic fields using nitrogen-vacancy centers in diamond," *Phys. Rev. Lett.*, vol. 103, p. 220802, 2009.
- [16] J. Achard, F. Silva, R. Issaoui, O. Brinza, A. Tallaire, H. Schneider, K. Isoird, H. Ding, S. Koné, M. A. Pinault, F. Jomard, and A. Gicquel, "Thick boron doped diamond single crystals for high power electronics," *Diam. Relat. Mater.*, vol. 20, p. 145, 2011.
- [17] F. Peter, "ber Brechungsindizes und Absorptionskonstanten des Diamanten zwischen 644 und 226 m?," *Zeitschrift für Physik*, vol. 15, p. 358, 1923.
- [18] A. M. Zaitsev, *Optical Properties of Diamond: A Data Handbook*, Berlin, Springer Science & Business Media, 2013.
- [19] P. Rath, S. Ummethala, C. Nebel, and W. H. P. Pernice, "Diamond as a material for monolithically integrated optical and optomechanical devices," *Phys. Status Solidi*, vol. 212, p. 2385, 2015.
- [20] E. Anoikin, A. Muhr, A. Bennett, D. Twitchen, and H. de Witin, "Diamond optical components for high-power and high-energy laser applications," *Int. Soc. Opt. Photonics*, p. 93460T, 2015, <https://doi.org/10.1117/12.2079714>.
- [21] A. Taylor, P. Ashcheulov, P. Hubík, L. Klimsa, J. Kopeček, Z. Remeš, Z. Vlčková Živcová, M. Remzová, L. Kavan, E. Scheid, J. Lorinčík, V. Mortet, "Precursor gas composition optimisation for large area boron doped nano-crystalline diamond growth by MW-LA-PECVD," *Carbon*, vol. 128, pp. 164–171, 2018. In press.
- [22] H. R. Phillip and E. A. Taft, "Kramers-Kronig analysis of reflectance data for diamond," *Phys. Rev.*, vol. 136, p. A1445, 1964.
- [23] H. H. Li, "Refractive index of silicon and germanium and its wavelength and temperature derivatives," *J. Phys. Chem. Ref. Data*, vol. 9, p. 561, 1980.
- [24] I. H. Malitson, "Refraction and dispersion of synthetic sapphire," *J. Opt. Soc. Am, JOS A*, vol. 52, p. 1377, 1962.
- [25] I. H. Malitson, "Interspecimen comparison of the refractive index of fused silica\*,†," *J. Opt. Soc. Am, JOS A*, vol. 55, p. 1205, 1965.
- [26] B. Bhushan and X. Li, "Micromechanical and tribological characterization of doped single-crystal silicon and polysilicon films for microelectromechanical systems devices," *J. Mater. Res.*, vol. 12, p. 54, 1997.
- [27] T. Chudoba, P. Schwaller, R. Rabe, J.-M. Breguet, and J. Michler, "Comparison of nanoindentation results obtained with Berkovich and cube-corner indenters," *Philos. Mag.*, vol. 86, p. 5265, 2006.
- [28] P. Hess, "The mechanical properties of various chemical vapor deposition diamond structures compared to the ideal single crystal," *J. Appl. Phys.*, vol. 111, p. 051101, 2012.
- [29] T. Schuelke and T. A. Grotjohn, "Diamond polishing," *Diam. Relat. Mater.*, vol. 32, p. 17, 2013.
- [30] M.-L. Hicks, A. C. Pakpour-Tabrizi, and R. B. Jackman, "Polishing, preparation and patterning of diamond for device applications," *Diam. Relat. Mater.*, vol. 97, p. 107424, 2019.
- [31] J. Schmitt, W. Nelissen, U. Wallrabe, and F. Völklein, "Implementation of smooth nanocrystalline diamond microstructures by combining reactive ion etching and ion beam etching," *Diam. Relat. Mater.*, vol. 79, p. 164, 2017.
- [32] S. Mi, A. Toros, T. Graziosi, and N. Quack, "Non-contact polishing of single crystal diamond by ion beam etching," *Diam. Relat. Mater.*, vol. 92, p. 248, 2019.
- [33] T. V. Kononenko, D. N. Sovyk, P. A. Pivovarov, V. S. Pavelyev, A. V. Mezhenin, K. V. Cherepanov, M. S. Komlenok, V. R. Sorochenko, A. A. Khomich, V. P. Pashinin, E. E. Ashkinazi, V. G. Ralchenko, and V. I. Konov, "Fabrication of diamond diffractive optics for powerful CO2 lasers via replication of laser microstructures on silicon template," *Diam. Relat. Mater.*, vol. 101, p. 107656, 2020.
- [34] H. A. Atikian, A. Eftekharian, A. Jafari Salim, M. J. Burek, J. T. Choy, A. Hamed Majedi, and M. Lončar "Superconducting nanowire single photon detector on diamond," *Appl. Phys. Lett.*, vol. 104, p. 122602, 2014.
- [35] Private communication with industrial partners.
- [36] J. Heupel, N. Felgen, R. Merz, M. Kopnarski, J. P. Reithmaier, and C. Popov, "Development of a planarization process for the fabrication of nanocrystalline diamond based photonic structures," *Phys. Status Solidi*, vol. 216, p. 1970072, 2019.
- [37] M. Rabarot, J. Widiez, S. Saada, J.-P. Mazellier, C. Lecouvey, J.-C. Roussin, J. Dechamp, P. Bergonzo, F. Andrieu, O. Faynot, S. Deleonibus, L. Clavelier, and J. P. Roger, "Silicon-on-diamond layer integration by wafer bonding technology," *Diam. Relat. Mater.*, vol. 19, p. 796, 2010.
- [38] M. Kiss, T. Graziosi, A. Toros, T. Scharf, C. Santschi, O. J. F. Martin, and N. Quack, "High-quality single crystal diamond diffraction gratings fabricated by crystallographic etching," *Opt. Express*, vol. 27, p. 30371, 2019.
- [39] T. Wildi, M. Kiss, and N. Quack, "Diffractive optical elements in single crystal diamond," *Opt. Lett.*, vol. 45, p. 3458, 2020.
- [40] A. Toros, N. Restori, M. Kiss, T. Scharf, and N. Quack, "Single crystal diamond blazed diffraction gratings and Fresnel microlens arrays with improved optical performance by high-resolution 3D laser lithography and pattern transfer by dry etching," *OSA Continuum, OSAC*, vol. 2, p. 3374, 2019.
- [41] S. Hatefi and K. Abou-El-Hossein, "Review of single-point diamond turning process in terms of ultra-precision optical surface roughness," *Int. J. Adv. Manuf. Technol.*, vol. 106, p. 2167, 2020.
- [42] K.-M. Tsai, "Effect of injection molding process parameters on optical properties of lenses," *Appl. Opt.*, vol. 49, p. 6149, 2010.
- [43] S. Antipov, S. V. Baryshev, J. E. Butler, O. Antipova, Z. Liu, and S. Stoupin, "Single-crystal diamond refractive lens for focusing X-rays in two dimensions," *J. Synchrotron Radiat.*, vol. 23, p. 163, 2016.
- [44] M. Karlsson, I. Vartianen, M. Kuittinen, and F. Nikolajeff, "Fabrication of sub-micron high aspect ratio diamond structures with nanoimprint lithography," *Microelectron. Eng.*, vol. 87, p. 2077, 2010.

- [45] J.-H. Seo, J. H. Park, S.-I. Kim, B. J. Park, Z. Ma, J. Choi, and B.-K. Ju, "Nanopatterning by laser interference lithography: applications to optical devices," *J. Nanosci. Nanotechnol.*, vol. 14, p. 1521, 2014.
- [46] P.-M. Coulon, B. Damilano, B. Alloing, P. Chausse, S. Walde, J. Enslin, R. Armstrong, S. Vézian, S. Hagedorn, T. Wernicke, J. Massies, J. Zúñiga-Pérez, M. Weyers, M. Kneissl, and P. A. Shields, "Displacement Talbot lithography for nano-engineering of III-nitride materials," *Microsyst. Nanoeng.*, vol. 5, p. 1, 2019.
- [47] A. Toros, M. Kiss, T. Graziosi, S. Mi, R. Berrazouane, M. Naamoun, J. Vukajlovic Plestina, P. Gallo, and N. Quack, "Reactive ion etching of single crystal diamond by inductively coupled plasma: State of the art and catalog of recipes," *Diam. Relat. Mater.*, p. 107839, 2020, <https://doi.org/10.1016/j.diamond.2020.107839>.
- [48] M. Karlsson and F. Nikolajeff, "Diamond micro-optics: microlenses and antireflection structured surfaces for the infrared spectral region," *Opt. Express*, vol. 11, p. 502, 2003.
- [49] Y. Fu and B. K. A. Ngoi, "Investigation of diffractive optical element fabricated on diamond film by use of focused ion beam direct milling," *Opt. Eng.*, vol. 42, p. 2214, 2003.
- [50] P. Forsberg and M. Karlsson, "Investigation of diffractive optical element fabricated on diamond film by use of focused ion beam direct milling," *Diam. Relat. Mater.*, vol. 34, p. 19, 2013.
- [51] M. Martínez-Calderon, J. J. Azkona, N. Casquero, A. Rodríguez, M. Domke, M. Gómez-Aranzadi, S. M. Olaizola, and E. Granados, "Tailoring diamond's optical properties via direct femtosecond laser nanostructuring," *Sci. Rep.*, vol. 8, p. 14262, 2018.
- [52] M. Karlsson and F. Nikolajeff, "Fabrication and evaluation of a diamond diffractive fan-out element for high power lasers," *Opt. Express*, vol. 11, p. 191, 2003.
- [53] E. Vargas Catalan, P. Forsberg, O. Absil, and M. Karlsson, "Controlling the profile of high aspect ratio gratings in diamond," *Diam. Relat. Mater.*, vol. 63, p. 60, 2016.
- [54] C. Delacroix, P. Forsberg, M. Karlsson, D. Mawet, O. Absil, C. Hanot, J. Surdej, and S. Habraken, "Design, manufacturing, and performance analysis of mid-infrared achromatic half-wave plates with diamond subwavelength gratings," *Appl. Opt.*, vol. 51, p. 5897, 2012.
- [55] P. Forsberg, M. Malmström, E. V. Catalan, and M. Karlsson, "Diamond grating waveplates," *Opt. Mater. Express*, vol. 6, p. 2024, 2016.
- [56] E. V. Catalán, P. Piron, A. Jolivet, P. Forsberg, C. Delacroix, E. Huby, O. Absil, I. Vartiainen, M. Kuittinen, and M. Karlsson, "Subwavelength diamond gratings for vortex coronagraphy: towards an annular groove phase mask for shorter wavelengths and topological charge 4 designs," *Opt. Mater. Express*, vol. 8, p. 1976, 2018.
- [57] F. Gao, Z. Huang, B. Feigel, J. Van Erps, H. Thienpont, R. G. Beausoleil, and N. Vermeulen, "Low-loss millimeter-length waveguides and grating couplers in single-crystal diamond," *J. Lightwave Technol.*, vol. 34, p. 5576, 2016.
- [58] G. Huszka, N. Malpiece, M. Naamoun, A. Mereuta, A. Caliman, G. Suruceanu, P. Gallo, and N. Quack, "Single crystal diamond gain mirrors for high performance vertical external cavity surface emitting lasers," *Diam. Relat. Mater.*, vol. 104, p. 107744, 2020.
- [59] M.-L. Hicks, A. C. Pakpour-Tabrizi, and R. B. Jackman, "Diamond etching beyond 10  $\mu\text{m}$  with near-zero micromasking," *Sci. Rep.*, vol. 9, p. 15619, 2019.
- [60] J. P. Hugonin and P. Lalanne, *Reticolo Software for Grating Analysis*, Orsay, Institut d'Optique, 2005.
- [61] M. Kiss, T. Graziosi, N. Quack, "Demonstration of V-groove diffraction gratings in single crystal diamond," *International Conference on Diamond and Carbon Materials, Gothenburg*, 2017.
- [62] M. Kiss, T. Graziosi, and N. Quack, "Trapezoidal diffraction grating beam splitters in single crystal diamond," *Proc. SPIE*, vol. 10513, p. 10513, 2018.
- [63] L. Li, E. H. Chen, J. Zheng, S. L. Mouradian, F. Dolde, T. Schröder, S. Karaveli, M. L. Markham, D. J. Twitchen, and D. Englund, "Efficient photon collection from a nitrogen vacancy center in a circular Bullseye grating," *Nano Lett.*, vol. 15, p. 1493, 2015.
- [64] F. Gao, J. V. Erps, Z. Huang, H. Thienpont, R. G. Beausoleil, and N. Vermeulen, "Down-scaling grating couplers and waveguides in single-crystal diamond for VIS-UV operation," *J. Phys. Photonics*, vol. 1, p. 015003, 2018.
- [65] M. Karlsson, K. Hjort, and F. Nikolajeff, "Transfer of continuous-relief diffractive structures into diamond by use of inductively coupled plasma dry etching," *Opt. Lett.*, vol. 26, p. 1752, 2001.
- [66] M. Makita, P. Karvinen, V. A. Guzenko, N. Kujala, P. Vagovic, and C. David, "Fabrication of diamond diffraction gratings for experiments with intense hard X-rays," *Microelectron. Eng.*, vol. 176, p. 75, 2017.
- [67] N. Kujala, M. Makita, J. Liu, A. Zozulya, M. Sprung, C. David, and J. Grünert, "Characterizing transmissive diamond gratings as beam splitters for the hard X-ray single-shot spectrometer of the European XFEL," *J. Synchrotron Radiat.*, vol. 26, p. 708, 2019.
- [68] A. L. Stepanov, V. I. Nuzhdin, M. F. Galyautdinov, N. V. Kurbatova, V. F. Valeev, V. V. Vorobev, and Yu. N. Osin, "A diffraction grating created in diamond substrate by boron ion implantation," *Tech. Phys. Lett.*, vol. 43, p. 104, 2017.
- [69] J. F. Ziegler, M. D. Ziegler, and J. P. Biersack, "SRIM: the stopping and range of ions in matter," *Nucl. Instrum. Methods Phys. Res. Sect. B Beam Interact. Mater. Atoms*, vol. 268, p. 1818, 2010.
- [70] F. Uhlén, D. Nilsson, A. Holmberg, H. M. Hertz, C. G. Schroer, F. Seiboth, J. Patommel, V. Meier, R. Hoppe, A. Schropp, H. J. Lee, B. Nagler, E. Galtier, J. Krzywinski, H. Sinn, and U. Vogt, "Damage investigation on tungsten and diamond diffractive optics at a hard x-ray free-electron laser," *Opt. Express*, vol. 21, p. 8051, 2013.
- [71] C. David, S. Gorelick, S. Rutishauser, J. Krzywinski, J. Vila-Comamala, V. A. Guzenko, O. Bunk, E. Färm, M. Ritala, M. Cammarata, D. M. Fritz, R. Barrett, L. Samoylova, J. Grünert, and H. Sinn, "Nanofocusing of hard X-ray free electron laser pulses using diamond based Fresnel zone plates," *Sci. Rep.*, vol. 1, p. 57, 2011.